Journal of Magnetism and Magnetic Materials 500 (2020) 166374

Contents lists available at ScienceDirect

Journal of Magnetism and Magnetic Materials

journal homepage: www.elsevier.com/locate/jmmm

Research articles

Magnetic structure of $ErFe_3(BO_3)_4$: Spectroscopic and thermodynamic studies

E.A. Popova[a,*], E.P. Chukalina[b,c], K.N. Boldyrev[b,c], A. Jablunovskis[c], I.A. Gudim[d]

[a] National Research University Higher School of Economics, Moscow 101000, Russia
[b] Institute of Spectroscopy, Russian Academy of Sciences, Troitsk, Moscow 108840, Russia
[c] Moscow Institute of Physics and Technology (National Research University), Dolgoprudnyi 141701, Russia
[d] Kirenskiy Institute of Physics, Siberian Branch of RAS, Krasnoyarsk 660036, Russia

ARTICLE INFO

Keywords:
Erbium iron borate
High-resolution optical spectroscopy
Modeling of magnetic properties

ABSTRACT

We report on the high-resolution spectroscopic study of multiferroic $ErFe_3(BO_3)_4$. The energies of all eight Kramers doublets of the ground $^4I_{15/2}$ multiplet of the Er^{3+} ion were determined by the high-resolution $^4I_{13/2} \rightarrow {}^4I_{15/2}$ infrared luminescence spectra. The spectroscopically determined temperature dependence of the splitting of the ground Kramers doublet was used to calculate the contribution of the erbium subsystem into the specific heat and the magnetic susceptibility of erbium iron borate. The analysis of the thermodynamic properties based on these calculations allowed us to suggest the domain structure in the easy-plane antiferromagnetically ordered iron subsystem, with two magnetically nonequivalent erbium positions in each domain.

1. Introduction

The erbium iron borate belongs to the family of multiferroic rare-earth (RE) iron borates $RFe_3(BO_3)_4$ (R = Y, La-Er) possessing the trigonal structure of the natural mineral huntite (space symmetry group $R32$ [1]). Magnetoelectric (ME) multiferroic properties of the RE iron borates were discovered and studied in a number of papers (see, e.g., Refs. [2–4]). The largest ME effect was observed in neodymium and samarium iron borates, in a magnetic field of 1 T values of 400 [2] and 500 μC/m^2 [3], respectively, were registered. $TbFe_3(BO_3)_4$ demonstrated a significant quadratic ME effect at room temperature, the value of which exceeded the value observed for the high-temperature multiferroic $BiFeO_3$. The effect changed its sign at a rotation of the magnetic field by 90° [5]. Such multiferroic materials have a potential for applications in ME sensors, magnetic switches, high-speed magnetoresistive random-access memory (MRAM), spintronic devices.

Like neodymium and samarium iron borates, erbium iron borate $ErFe_3(BO_3)_4$ is an easy-plane magnet. It was expected to find large values of the ME effect in it, similar to those registered in $NdFe_3(BO_3)_4$ and $SmFe_3(BO_3)_4$. However, in magnetic fields up to 10 T, the electric polarization in $ErFe_3(BO_3)_4$ turned out to be negligible — less than 5 μC/m^2 [4]. The authors of [4] suggested that the magnitude of the ME effect depends on the type of the RE ion, in particular, on the characteristics of its electronic structure. Detailed knowledge of the magnetic structure also can be important. Based on neutron scattering results, Ref. [6] reported an easy-plane antiferromagnetic arrangement of magnetic moments below T_N = 39 K, however, not only a collinear one, like in $NdFe_3(BO_3)_4$ and $SmFe_3(BO_3)_4$, but also a 120° one for erbium magnetic moments at temperatures below 10 K. Thus, information on electronic crystal-field (CF) levels of the ground Er^{3+} multiplet as well as on magnetic structure of $ErFe_3(BO_3)_4$ in a magnetically ordered phase is topical for understanding ME properties of this compound.

As for the CF levels of the ground Er^{3+} multiplet ($^4I_{15/2}$) in $ErFe_3(BO_3)_4$, contradictory results were published [7,8]. The magnetic structure could be clarified by neutron scattering experiments on single crystals of $ErFe_3(BO_3)_4$. Another way to refine it is to model thermodynamic characteristics of the compound. Magnetic susceptibility and specific heat of $ErFe_3(BO_3)_4$ single crystals were experimentally measured in Ref. [9]. However, a simulation of the temperature dependences of these thermodynamic quantities [9] was performed not taking into account spectroscopic data on $ErFe_3(BO_3)_4$. For a correct modeling, the CF structure of the $^4I_{15/2}$ ground multiplet is, again, essential.

In Refs. [7,8], the CF structure of the $^4I_{15/2}$ ground multiplet was determined from the absorption spectra at elevated temperatures when excited CF levels are populated. Due to the temperature broadening of spectral lines in complicated spectra consisting of a great number of lines, this determination is difficult to make precisely. Much more precise data on the CF structure of the ground multiplet can be

* Corresponding author at: National Research University Higher School of Economics, 20, Myasnitskaya Str., Moscow 101000, Russia.
E-mail address: eapopova@hse.ru (E.A. Popova).

https://doi.org/10.1016/j.jmmm.2019.166374
Received 1 August 2019; Received in revised form 21 December 2019; Accepted 29 December 2019
Available online 31 December 2019
0304-8853/

extracted from the low-temperature luminescence spectra. To solve the existing ambiguity in the CF structure of the ground multiplet $^4I_{15/2}$ of Er^{3+} in $ErFe_3(BO_3)_4$, we decided to search for a luminescence, which was not explored before because of a supposed strong quenching in this concentrated in Er and Fe compound [10]. Our efforts have been crowned with success.

Here, we report on a high-resolution temperature-dependent spectroscopic study of the infrared luminescence of newly grown high-quality single crystals of erbium iron borate. A thorough analysis of the $^4I_{13/2} \rightarrow {}^4I_{15/2}$ spectra allowed us to establish unambiguously the energies of the CF levels of the $^4I_{15/2}$ ground multiplet of Er^{3+} in $ErFe_3(BO_3)_4$. Below $T_N = 39$ K the erbium Kramers doublets split in an internal magnetic field created by ordered iron magnetic moments. We have determined the temperature dependence of these splittings by analyzing high-resolution $^4I_{15/2} \rightarrow {}^4I_{13/2}$ absorption spectra. We use the obtained results to model the literature data [9] on the thermodynamic properties of the compound. A magnetic structure compatible with these results is suggested.

2. Materials and methods

The RE iron borates melt incongruently and single crystals are grown by the solution-melt method [1]. It should be noted that in the series of RE iron borates, the $ErFe_3(BO_3)_4$ compound is the last to be grown as single crystals. In this connection, the problem arises of improving the technology of growing high-quality single crystals with the subsequent characterization of the samples obtained.

For these studies, we have elaborated a special technology for growing single crystals of the erbium iron borate. The following composition of the solution-melt was selected:

76.7 wt% [$Bi_2Mo_3O_{12}$ + $3.15B_2O_3$ + $0.6Er_2O_3$] + 23.3 wt% $ErFe_3(BO_3)_4$. The saturation temperature of this solution-melt was 940 ± 3 °C. A two-stage spontaneous crystallization during 24 h resulted in single crystals with dimensions up to 1 mm^3, which were used as seeds. The growth of large high-quality crystals from so obtained seeds placed onto rotating holders continued for 89 days in an oven with software controlled temperature. More details on the technology will be published elsewhere.

Samples with a thickness of 2.016 and 0.15 mm were cut perpendicular and, respectively, parallel to the crystallographic *c* axis and polished. A Fourier spectrometer Bruker IFS125HR with an InSb liquid-nitrogen-cooled detector and a closed-helium-cycle cryostat Cryomech ST403 were used to register the infrared luminescence and transmission spectra in the spectral range 5000–9000 cm^{-1} with a resolution down to 0.2 cm^{-1} in a broad range of temperatures (10–300 K). The luminescence was excited by a diode laser with the wave length λ = 450 nm.

3. Spectroscopic results on the crystal-field levels of the ground multiplet $^4I_{15/2}$ of Er^{3+} in $ErFe_3(BO_3)_4$

The erbium iron borate crystallizes in the *R*32 space group with a single D_3 symmetry position for the Er^{3+} ion. At $T_s = 431$ K, i.e., well above the room temperature, the compound undergoes a structural phase transition into the $P3_121$ phase [11,7], wherein the symmetry of the erbium site lowers from the D_3 point group to the C_2 one. In the crystal field of such symmetry, the $^{2S+1}L_J$ levels of the free Er^{3+} ion split into (2 *J* + 1)/2 Kramers doublets characterized by the Γ_{34} irreducible representation of the C_2 point symmetry group.

In Ref. [7], some of us have determined the energies of the CF levels of the two lowest CF manifolds of $ErFe_3(BO_3)_4$, namely, of $^4I_{15/2}$ and $^4I_{13/2}$, from the analysis of the high-resolution temperature-dependent optical transmission spectra in the infrared region between 6000 and 7000 cm^{-1}. The obtained data are given in Table 1. Independently, Ref. [8] reported differing data on the structure of the ground multiplet $^4I_{15/2}$, derived from the analysis of the π- and σ-polarized absorption spectra of $ErFe_3(BO_3)_4$ at $T = 90$ K in the spectral region 9000–23000 cm^{-1}. To check our data of Ref. [7] on $^4I_{15/2}$, we have performed high-resolution temperature-dependent measurements of the infrared luminescence spectra in the region of the $^4I_{13/2} \rightarrow {}^4I_{15/2}$ transition (6000–7000 cm^{-1}) of $ErFe_3(BO_3)_4$ in the low-symmetry $P3_121$ structural phase (10–300 K).

Table 1
Energies (cm^{-1}) of CF levels of the Er^{3+} ion in $ErFe_3(BO_3)_4$, according to our high-resolution transmission and luminescence data ([7], this work).

$^4I_{15/2}$	[7], this work	0	46	105	160	194	244	279	296
$^4I_{13/2}$	[7]	6539	6573	6623	6639	6684	6714	6723	

Fig. 1a shows the luminescence spectra of $ErFe_3(BO_3)_4$ at the two temperatures, 150 and 10 K (measured at the sample holder). The notation of a given spectral line acquires notations of both the initial and final level of an optical transition, wherein the CF levels of the ground (excited) multiplet are designated by numbers (capital letters), as it is shown at the scheme of Fig. 1b. With lowering temperature, the spectral lines narrow (but shift very little) and some of them disappear, because of depopulation of the initial levels of optical transitions (G, F, etc. in Fig. 1b). The presence of the lines originating from the levels B, C, and even D in the low-temperature spectra can be explained by two reasons, namely, (i) a slow relaxation to the lowest-energy level of the $^4I_{13/2}$ CF manifold, due to a low density of the lattice phonon states at energies equal to the differences $E_B - E_A$, $E_C - E_A$, etc. (the so-called hot luminescence) and (ii) heating of the sample by the excitation laser light. Whatever the reason is, it does not prevent us from an unambiguous identification of the spectral lines. In Fig. 1, positions of the spectral lines A1, A2, …, B1, etc. calculated from the absorption data of Ref. [7] (Table 1) are shown. An excellent agreement between our absorption and luminescence data can be seen. In Fig. 1, we have also plotted expected positions of the luminescence lines in the case of the CF levels of the ground multiplet suggested in Ref. [8] (A1′, A2′, etc.). Wrong energy values for the levels 4′, 5′, 6′, and 7′ of Ref. [8] are evident.

Thus, by analyzing the high-resolution infrared luminescence spectra of $ErFe_3(BO_3)_4$, we have confirmed the CF levels' scheme for the $^4I_{15/2}$ ground multiplet of the Er^{3+} ion determined earlier from the absorption spectra [7] and removed an ambiguity in the literature data.

4. Spectroscopic results on the temperature dependence of the Er^{3+} ground-state splitting in a magnetically ordered phase of $ErFe_3(BO_3)_4$

At $T_N = 39$ K, $ErFe_3(BO_3)_4$ orders into an easy-plane antiferromagnetic structure [12,4,9] and this phase transition is accompanied by a splitting of the CF Kramers doublets [12]. As a result, each spectral line splits, in a general case, into four components (as is evident from the scheme of Inset in Fig. 2b). Fig. 2a shows the 1B absorption line of the $^4I_{15/2} \rightarrow {}^4I_{13/2}$ optical transition at different temperatures. Components of the split line are labeled according to the notations adopted in the mentioned scheme. Due to a relatively large line widths, the 1′b″ and 1″b′ components are present as shoulders at the high- and low-frequency side of the line, respectively. Lines originating from the upper level 1″ of the split ground Kramers doublet diminish in intensity with decreasing temperature, due to depopulation of the 1″ level. The exchange splitting of the ground Kramers doublet $\Delta_0(5\text{ K}) = 6.3 \pm 1$ cm^{-1} follows from the analysis of the shape of the line 1B at $T = 5$ K [7]. Fig. 2b demonstrates the temperature dependence of the Er^{3+} ground-state splitting in $ErFe_3(BO_3)_4$ obtained from the analysis of high-resolution absorption spectra and compares it with the temperature dependence of iron magnetic moments measured in neutron scattering experiments [6]. Proportionality of these two physical quantities testifies a decisive role of the Er – Fe interaction in the splitting of erbium Kramers doublets.

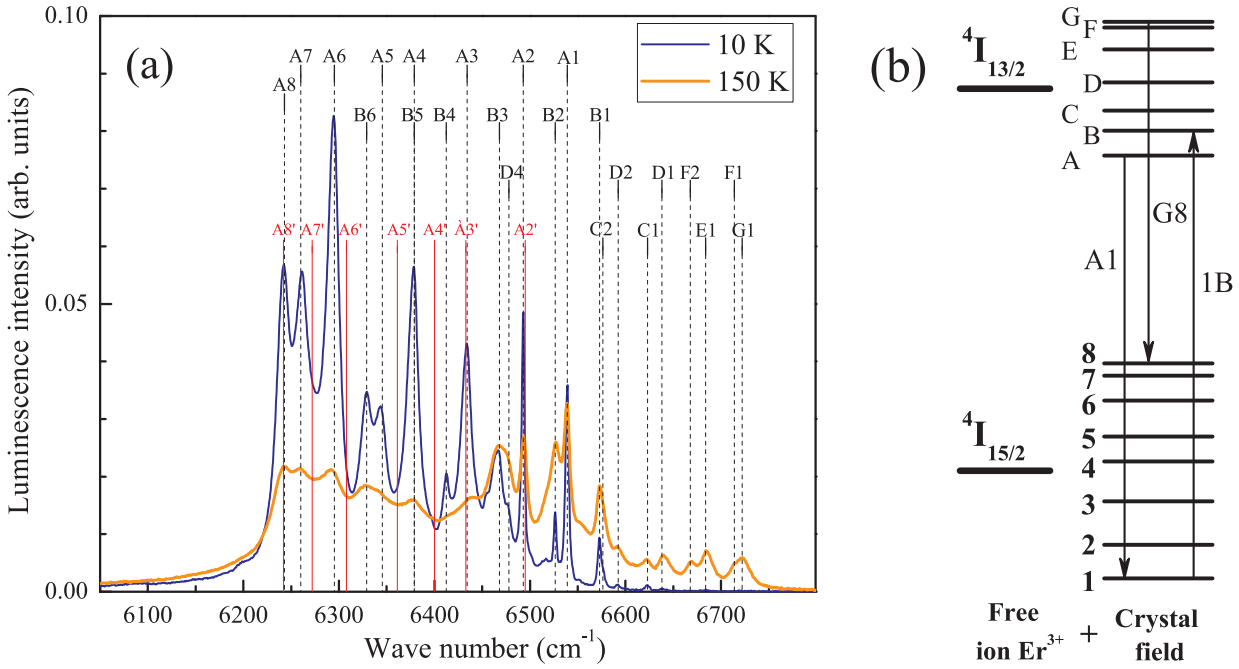

Fig. 1. (a) The luminescence spectra of 2.016 mm thick $ErFe_3(BO_3)_4$ sample in the region of the $^4I_{13/2} \rightarrow {}^4I_{15/2}$ optical transition of the Er^{3+} ion and (b) the scheme of the CF levels of the two lowest-energy multiplets of Er^{3+} in $ErFe_3(BO_3)_4$. Arrows show some of the transitions observed in the luminescence (A1, G8) and absorption (1B) spectra. Hatching notations in (a) refer to the line positions calculated with the data of Ref. [8].

In the following sections, we use these spectroscopic data to simulate the temperature dependences of the specific heat and magnetic susceptibility of $ErFe_3(BO_3)_4$ single crystals, which have been reported in the literature [9].

5. Specific heat of $ErFe_3(BO_3)_4$: Simulation of the Schottky anomaly. The domain structure of the ordered iron subsystem

Fig. 3 presents the temperature dependence of the specific heat $C(T)$ of $ErFe_3(BO_3)_4$ [9]. A sharp λ-type anomaly at 38 K corresponds to a second-order magnetic phase transition into an antiferromagnetic structure of the iron magnetic moments [9]. The Schottky anomaly observed in the specific heat data around 3 K is due to the temperature-

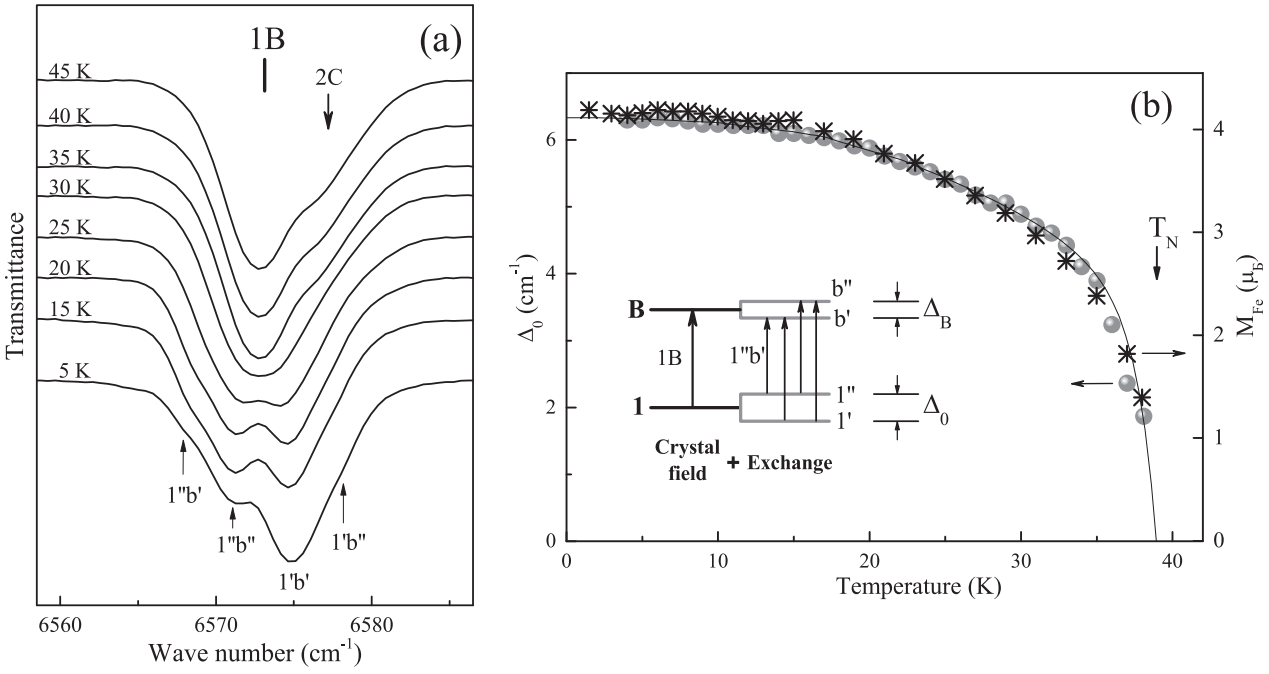

Fig. 2. (a) Absorption line 1B in the spectrum of $ErFe_3(BO_3)_4$ (see the scheme of Fig. 1b) at different temperatures. Components of the lines split in a magnetically ordered state are labeled according to the scheme presented as Inset of Fig. 2b. (b) Temperature dependences of the ground-state splitting and of the magnetic moment of iron ions in $ErFe_3(BO_3)_4$ measured in neutron scattering experiments [6]. Inset: the scheme of exchange splittings of the Kramers doublets in a magnetically ordered state.

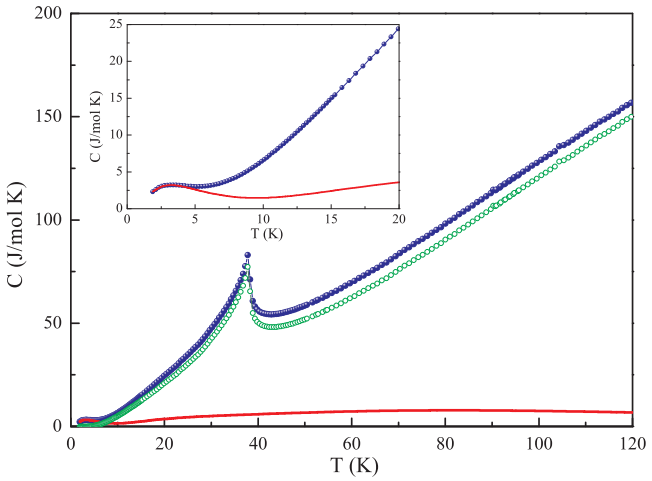

Fig. 3. The temperature dependence of the specific heat of $ErFe_3(BO_3)_4$. Blue filled symbols refer to the experimental data [9]. A red solid line is a contribution of the erbium subsystem to the specific heat calculated from the spectroscopic data. Green open symbols represent the experimental data minus the contribution of the rare-earth subsystem. Inset highlights the temperature range below 20 K. The simulation was performed under the assumption of two magnetically nonequivalent Er positions. (see the text). (For interpretation of the references to colour in this figure legend, the reader is referred to the web version of this article.)

driven depopulation of the upper sublevel of the ground Kramers doublet of the Er^{3+} ion split by an internal magnetic field appearing at the magnetic ordering.

In Ref. [9], the contribution of the erbium subsystem into the specific heat was calculated taking into account only the ground Kramers doublet of the Er^{3+} ion. Here, we perform calculations considering all eight Kramers doublets of the ground state of the Er^{3+} ion, according to the formula:

$$C(T) = R \cdot \frac{(\sum_i x_i^2 \cdot e^{-x_i}) \cdot (\sum_i e^{-x_i}) - (\sum_i x_i \cdot e^{-x_i})^2}{(\sum_i e^{-x_i})^2} \quad (1)$$

where R is the gas constant, $x_i = \frac{E_{i_0}}{kT} \pm \frac{\Delta_i}{2kT}$, k is the Boltzmann constant, E_{i_0} is the energy of the i-th Kramers doublet of the ground state in the absence of an internal magnetic field, Δ_i is the splitting of the i-th Kramers doublet in the internal field. We note that when modeling the Schottky anomaly with the maximum at 3 K, only the splitting of the ground Kramers doublet $\Delta_0(T)$ should be taken into account, since the population of all excited levels is negligible in this temperature range. In our calculations, we used the spectroscopically determined temperature dependence of the ground-state splitting $\Delta_0(T)$ (see Fig. 2b). The calculated contribution of erbium to the specific heat is shown by a solid line in Fig. 3, it occupies a wide temperature range up to 300 K and has a maximum in the region of 90 K. However, only at low temperatures the contribution of the erbium subsystem significantly exceeds the lattice contribution and results in an observable Schottky anomaly in the measured specific heat with the maximum at about 3 K.

The exchange splitting $\Delta_0 = 6.3 \pm 1\ cm^{-1}$ at 5 K was reported for the ground Kramers doublet from the analysis of high-resolution spectroscopic data [7]. However, we failed to fit well the experimentally observed Schottky anomaly in the $C(T)$ dependence of $ErFe_3(BO_3)_4$ when using this value: the maximum of the calculated curve was shifted to a higher temperature by about 1 K with respect to the experimental data and its value was slightly higher than the experimental one.

To find the reason of this discrepancy, we return to the information on the magnetic structure of $ErFe_3(BO_3)_4$ reported in Ref. [6] on the basis of neutron scattering experiments. Ref. [6] announced a collinear easy-plane antiferromagnetic structure of the ordered iron magnetic moments directed along the C_2 symmetry axis in the *ab* crystallographic plane of $ErFe_3(BO_3)_4$. In each *ab* layer, the ferromagnetic order of the iron magnetic moments takes place but the nearest layers are ordered antiferromagnetically (see Fig. 6 of Ref. [6]). Each Er^{3+} ion is connected through six oxygen ions, which form a distorted coordination prism, with six Fe^{3+} ions residing in the next-nearest layers and, thus, having equally directed magnetic moments. As a result, the erbium ion experiences an effective internal magnetic field (the exchange field B_{ex}) directed along these iron magnetic moments.

We note here that such structure implies an existence of the three types of domains, because there are three equivalent C_2 axes in the *ab* plane with the angle of 120° between them. In the $P3_121$ crystal structure of $ErFe_3(BO_3)_4$, there are three crystallographically equivalent but magnetically nonequivalent erbium sites (Er1, Er2, and Er3) described by the C_2 point symmetry group, with their C_2 axes along one of the three C_2 symmetry axes of the crystal. In the case of a domain of a collinear structure of the Fe magnetic moments, one of these Er ions, e.g., Er1, experiences an internal magnetic field directed along its C_2 axis, while Er2 and Er3 are subjected to a magnetic field at the angles ± 120° respective to their local C_2 axes (see the scheme of Fig. 4 for the domain 1) and, thus, one should await different Zeeman splittings of the Kramers doublets, Δ_1 for Er1 and $\Delta_2 = \Delta_3$ for Er2 and Er3.

The Zeeman splitting of Kramers doublet of a given erbium ion in a magnetic field (which is the sum B of both an external magnetic field B_0 and an internal exchange one B_{ex}) reads:

$$\Delta = \mu_B [(B_x g_{xx})^2 + (B_y g_{yy})^2 + (B_y g_{yz} + B_z g_{zz})^2]^{1/2} \quad (2)$$

where μ_B is the Bohr magneton, g_{ij} are the g-tensor components (i,j = x, y, z) for a considered Kramers doublet of the ground multiplet of the Er^{3+} ion; B_i is the component of the magnetic field; $B_i = B\cos\phi_i$ where $\phi_i = \alpha, \beta, \gamma$ are the angles between the direction of the magnetic field and the local x,y,z axes of a given erbium ion, respectively (the z axis is directed along the crystallographic c axis and the x axis goes along the local C_2 symmetry axis).

Calculations have shown that the best agreement with the experimental $C(T)$ dependence is achieved if we assume that in the absence of

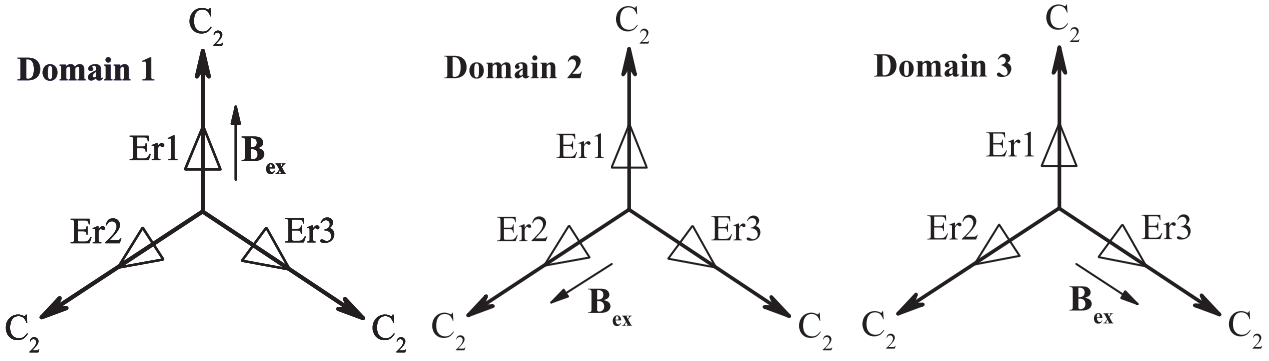

Fig. 4. The scheme clarifying magnetically nonequivalent erbium positions in a single magnetic domain. The C_2 symmetry axes lay in the *ab* plane of the crystal.

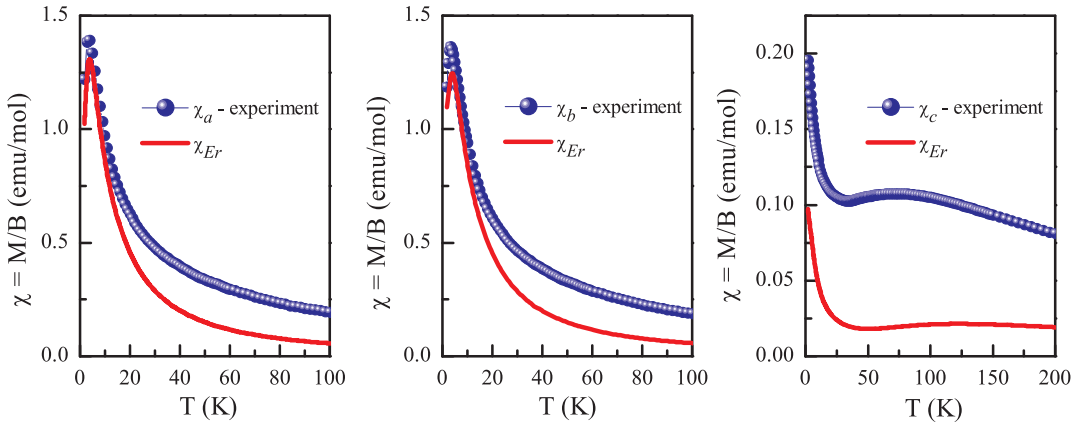

Fig. 5. Temperature dependence of the magnetic susceptibility of $ErFe_3(BO_3)_4$. The symbols represent the experimental data [9]. The solid line is a calculated contribution of the erbium subsystem to the magnetic susceptibility.

an external magnetic field the splitting of the ground Kramers doublet for one of the Er3 + ions (e.g., Er1) is $\Delta_1 = \Delta_0/2$, while for the other two (Er2 and Er3) it is $\Delta_2 = \Delta_3 = \Delta_0$. Substituting each of the values Δ_0 and $\Delta_0/2$ as well as the values $g_{xx} = 8.68$, $g_{yy} = 10.14$ [13] into Eq. (2), of the two obtained equations we find that $g_{yz} = 16.3$ and that the magnetic moments of the Fe^{3+} ions lie along one of the C_2 axes in the *ab* plane of the crystal within each domain The estimated internal magnetic field acting on the erbium subsystem is about $B_{ex} = 0.76$ T at 2 K. Thus simulated $C(T)$ curve is shown in Inset of Fig. 3. The above made assumption about two values of splitting Δ_1 and $\Delta_2 = \Delta_3$ does not contradict our spectroscopic data (Ref. [7] and this work). In the lowest-temperature optical spectra, the line shape is due to the splitting Δ_0 whereas the splitting $\Delta_0/2$ is hidden inside the inhomogeneous broadening of the line, which is rather large (see Fig. 2a).

6. Simulation of the magnetic susceptibility of $ErFe_3(BO_3)_4$. Considerations on the magnetic structure

In the magnetic susceptibility measurements, the external magnetic field $B_0 = 0.05$T was directed along the *a*, *b′*, and *c* axes of the crystal (the *b′* axis is perpendicular to the both *a* and *c* axes). First of all, we estimate the contribution of the iron subsystem into the magnetic susceptibility of $ErFe_3(BO_3)_4$. In the case of the magnetic field directed along the *c* axis, the antiferromagnetic vector of ordered iron magnetic moments in each domain remains perpendicular to the magnetic field and the total magnetic susceptibility of the iron subsystem $\chi_\perp$ is temperature independent below the Néel temperature. If the applied magnetic field is perpendicular to the *c* axis, each domain makes a different contribution to the magnetic susceptibility. In the case of $B_0||a$, the antiferromagnetic vector of one of the domains is parallel to the magnetic field, and the magnetic susceptibility of this domain amounts to $\chi_{||}$. The other two domains contribute a value equal to $(\chi_{||} + \sqrt{3}\chi_\perp)$, and the total magnetic susceptibility of the iron subsystem amounts to $\chi_a^{Fe} = \frac{1}{3}(2\chi_{||} + \sqrt{3}\chi_\perp)$. In the case of $B_0||b'$, $\chi_{b'}^{Fe} = \frac{1}{3}(\sqrt{3}\chi_{||} + 2\chi_\perp)$. Taking into account that $\chi_{||} = 0$ at $T = 0$ K and $\chi_{||} = \chi_\perp$ at $T = T_N$, we find that the magnetic susceptibility of the iron subsystem is $\chi_a^{Fe} = \frac{\sqrt{3}}{3}\chi_\perp$, $\chi_{b'}^{Fe} = \frac{2}{3}\chi_\perp$ at $T = 0$ K and $\chi_a^{Fe} = \chi_{b'}^{Fe} = \frac{1}{3}(2 + \sqrt{3})\chi_\perp$ at $T = T_N$. So, the total contribution of the iron subsystem into $\chi_a(T)$ and $\chi_{b'}(T)$ measured along the *a* and *b′* axes, respectively, is almost identical. The value of $\chi_\perp$ was estimated from the $\chi_c(T)$ dependence measured along the *c* axis: $\chi_\perp = \chi_c^{Fe} = 0.078\frac{\text{emu}}{\text{mol}}$.

Next, we consider the erbium contribution into the total magnetic susceptibility. In the presence of an external magnetic field in the *ab* plane, the effective magnetic field acting on the Er^{3+} ions is $B = B_0 + B_{ex}$. The splitting of Kramers doublets depends on the magnitude and direction of the effective magnetic field with respect to the local axes of each Er^{3+} ion. The contribution of the erbium subsystem into the total magnetic susceptibility can be defined as a sum of projections of the magnetic moment components for each Er^{3+} ion of each domain on the direction of the external magnetic field. The m_x and m_y components contribute to the total magnetic susceptibly in the case of the external magnetic fields $B_0||a$ and $B_0||b'$, whereas the m_z component should be taken into account in the case of $B_0||c$. Using Eq. (2) and taking into account the Boltzmann distribution for the population of the components of the split Kramers doublets, we find for each Kramers doublet of the ground erbium multiplet:

$$m_x = \mu_B^2 \frac{B_x g_{xx}^2}{2\Delta} th(\Delta/2kT)$$

$$m_y = \mu_B^2 \frac{B_y(g_{yy}^2 + g_{yz}^2) + B_z g_{yz} g_{zz}}{2\Delta} th(\Delta/2kT) \quad (3)$$

$$m_z = \mu_B^2 \frac{B_z g_{zz}^2 + B_y g_{yz} g_{zz}}{2\Delta} th(\Delta/2kT)$$

Note that the components of the magnetic moments refer to the local coordinate systems which are placed at the erbium sites. The modeling of the magnetic susceptibility of the erbium subsystem along the *a*, *b′*, and *c* axes was carried out with the use of Eqs. (3) taking into account the temperature-dependent populations of all eight Kramers doublets of the ground crystal-field multiplet of the Er^{3+} ions in magnetically nonequivalent positions in each domain and splitting of these doublets calculated according to Eq. (2) with *g* factors from [14]. The experimental data on the magnetic susceptibility and the calculated total contributions of the erbium subsystem are shown in Fig. 5.

Fig. 6 presents the moments of magnetically nonequivalent Er1, Er2, and Er3 ions in each domain at different temperatures in the zero external magnetic field, calculated with the help of Eqs. (3). For erbium ions with the splitting of the ground Kramers doublet equal to Δ_0, the direction of the magnetic moment slightly changes with temperature, whereas for the Er^{3+} ions possessing the splitting $\Delta_0/2$, the magnetic moments are directed along the *a* axis of the crystal at any temperature.

Fig. 7 displays the calculated temperature dependences of the magnetic moments of Er1, Er2, and Er3 ions in different domains in zero external magnetic field. These two curves are similar to those of Fig. 9 in Ref. [6] determined from neutron scattering experiments. However, in Ref. [6] the smallest magnetic moment was referred to the "120° structure" of the Er magnetic moments below 10 K. We argue that the lowest curve corresponds to the Er1, Er2, and Er3 in the domains 1, 2, and 3, respectively, with their C_2 symmetry axes along the direction of the iron magnetic moment in a given domain and with the same splitting of the ground Kramers doublet equal to $\Delta_0/2$. The highest curve in Fig. 7 represents six erbium ions with the same splitting Δ_0,

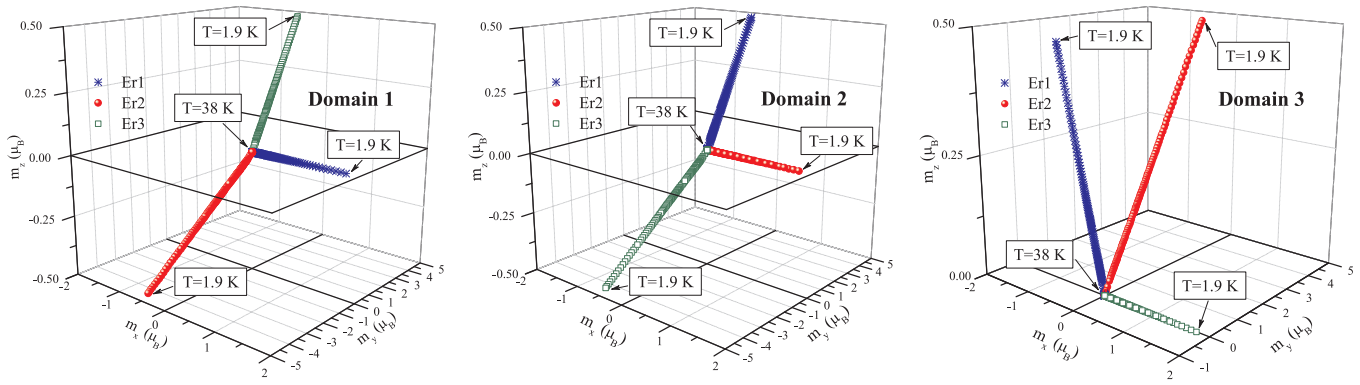

Fig. 6. The m_x, m_y, and m_z components of the magnetic moments of magnetically nonequivalent Er^{3+} ions in different domains at different temperatures.

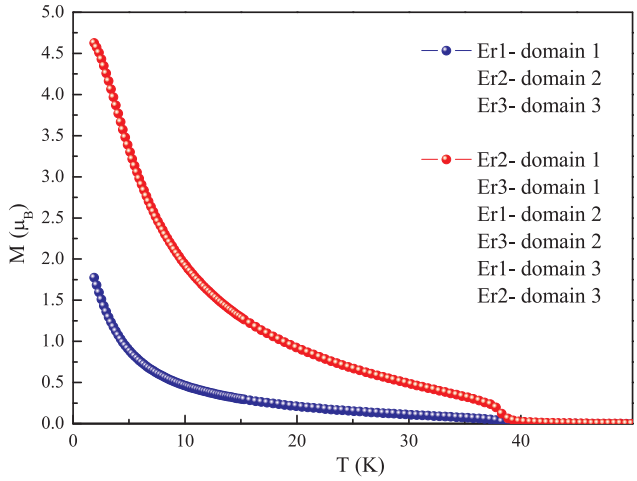

Fig. 7. The temperature dependences of the magnetic moments of the Er^{3+} ions. The lowest curve represents the total magnetic moment of the three Er ions with the same splitting of the ground Kramers doublet equal to $\Delta_0/2$ (Er1, Er2, and Er3 in the domains 1, 2, and 3, respectively). The highest curve represents the six Er ions possessing the splitting Δ_0 (Er1 in domains 2 and 3, Er2 in domains 1 and 3, and Er3 in domains 1 and 2).

namely, Er1 in domains 2 and 3, Er2 in domains 1 and 3 , and Er3 in domains 1 and 2 (See, Fig. 4).

7. Conclusions

Applying high-resolution temperature-dependent spectroscopic measurements, we have unambiguously established the energies of the crystal-field levels of the ground multiplet $^4I_{15/2}$ of Er^{3+} in $ErFe_3(BO_3)_4$ and derived the temperature dependence of the erbium ground Kramers doublet splitting in the magnetically ordered phase of $ErFe_3(BO_3)_4$. We used these data to simulate the experimentally measured temperature dependences of the specific heat and magnetic susceptibility of the erbium iron borate single crystals. The experimental data were well reproduced by calculations, which accounted for the existence of the three types of magnetic domains with a collinear easy-plane structure of the ordered iron magnetic moments in each of them and of magnetically nonequivalent positions of erbium. Based on these simulations, we suggested an alternative explanation to the "120° structure" of the Er magnetic moments in $ErFe_3(BO_3)_4$, announced in the neutron scattering study of Ref. [6] below 10 K, namely, the existence of 120° domains of collinear arrangement of the Fe magnetic moments along the C_2 symmetry axes (with the angle 120° between them) in the *ab* plane and two magnetically nonequivalent positions of Er^{3+} ions with different directions of their magnetic moments in different domains.

CRediT authorship contribution statement

E.A. Popova: Investigation, Visualization, Conceptualization, Writing - review & editing, Methodology, Formal analysis. **E.P. Chukalina:** Investigation, Visualization, Conceptualization, Writing - original draft. **K.N. Boldyrev:** Investigation. **A. Jablunovskis:** Investigation, Visualization. **I.A. Gudim:** Resources.

Declaration of Competing Interest

The authors declare that they have no known competing financial interests or personal relationships that could have appeared to influence the work reported in this paper.

Acknowledgments

E.P.Ch., and K.N.B. acknowledge a financial support of the Russian Science Foundation under Grant # 19-12-00413. The calculational part of the article was prepared by . E.A.P. within the framework of the Academic Fund Program at the National Research University Higher School of Economics (HSE University) in 2019 (grant №19-04-030) and by the Russian Academic Excellence Project «5-100».

References

[1] N.I. Leonyuk, L.I. Leonyuk, Growth and characterization of $RM_3(BO_3)_4$ crystals, Prog. Cryst. Growth Charact. Mater. 31 (1995) 179–278, https://doi.org/10.1016/0960-8974(96)83730-2.

[2] A.K. Zvezdin, G.P. Vorob'ev, A.M. Kadomtseva, YuF. Popov, A.P. Pyatakov, L.N. Bezmaternykh, A.V. Kuvardin, E.A. Popova, Magnetoelectric and magnetoelastic interactions in $NdFe_3(BO_3)_4$ multiferroics, JETP Lett. 83 (2006) 509–514, https://doi.org/10.1134/S0021364006110099.

[3] A.A. Mukhin, G.P. Vorob'ev, V.Yu Ivanov, A.M. Kadomtseva, A.S. Narizhnaya, A.M. Kuz'menko, Yu.F. Popov, L.N. Bezmaternykh, I.A. Gudim, Colossal magnetodielectric effect in $SmFe_3(BO_3)_4$ multiferroic, JETP Lett. 93 (2011) 275–281, https://doi.org/10.1134/S0021364011050079.

[4] A.M. Kadomtseva, Yu.F. Popov, G.P. Vorob'ev, A.P. Pyatakov, S.S. Krotov, K.I. Kamilov, V.Yu Ivanov, A.A. Mukhin, A.K. Zvezdin, A.M. Kuz'menko, L.N. Bezmaternykh, I.A. Gudim, V.L. Temerov, Magnetoelectric and magnetoelastic properties of rare-earth ferroborates, Low Temperature 511 (2010), https://doi.org/10.1063/1.3457390.

[5] A.K. Zvezdin, A.M. Kadomtseva, Yu.F. Popov, G.P. Vorob'ev, A.P. Pyatakov, V.Yu Ivanov, A.M. Kuz'menko, A.A. Mukhin, L.N. Bezmaternykh, I.A. Gudim, Magnetic anisotropy and magnetoelectric properties of $Tb_{1-x}Er_xFe_3(BO_3)_4$ ferroborates, JETP 109 (2009) 68–73, https://doi.org/10.1134/S1063776109070097.

[6] C. Ritter, A. Vorotynov, A. Pankrats, G. Petrakovski, V. Temerov, I. Gudim, R. Szymczak, Magnetic structure in iron borates $RFe_3(BO_3)_4$ (R = Er, Pr): a neutron diffraction and magnetization study, J. Phys.: Condens. Matter 22 (2010), https://doi.org/10.1088/0953-8984/22/20/206002.

[7] D. Erofeev, A. Jablunovskis, E. Chukalina, Optical spectroscopy of $ErFe_3(BO_3)_4$: detection of phase transitions and crystal-field levels of the Er^{3+} ground multiplet, EPJ Web Conf. 185 (2018) 07002, https://doi.org/10.1051/epjconf/201818507002.

[8] A.V. Malakhovskii, V.V. Sokolov, I.A. Gudim, Influence of the low local symmetry of Er^{3+} ions on magnetic circular dichroism and absorption spectra of f-f transitions in $ErFe_3(BO_3)_4$ single crystal, J. Magn. Magn. Mater. 465 (2018) 700–708, https://doi.org/10.1016/j.jmmm.2018.06.057.

[9] E.A. Popova, A.N. Vasiliev, V.L. Temerov, L.N. Bezmaternykh, N. Tristan, R. Klingeler, B. Buchner, Magnetic and specific heat properties of $YFe_3(BO_3)_4$ and $ErFe_3(BO_3)_4$, J. Phys.: Condens Matter 22 (2010), https://doi.org/10.1088/0953-8984/22/11/116006.

[10] A.V. Malakhovskii, A.L. Sukhachev, V.V. Sokolov, T.V. Kutsak, V.S. Bondarev, I.A. Gudim, Magneto-optical activity of f–f transitions in $ErFe_3(BO_3)_4$ and $ErAl_3(BO_3)_4$ single crystals, J. Magn. Magn. Mater. 384 (2015) 255–265, https://doi.org/10.1016/j.jmmm.2015.02.051.

[11] D. Fausti, A. Nugroho, P. van Loosdrecht, S.A. Klimin, M.N. Popova, L.N. Bezmaternykh, Raman scattering from phonons and magnons in $RFe_3(BO_3)_4$, Phys. Rev. B. 74 (2006) 024403, , https://doi.org/10.1103/PhysRevB.74.024403.

[12] M.N. Popova, E.P. Chikalina, T.N. Stanislavchuk, L.N. Bezmaternykh, Different types of magnetic ordering in $RFe_3(BO_3)_4$, R = Gd, Tb, Er, and Y, as studied by the method of Er^{3+} spectroscopic probe, J. Magn. Magn. Mater. 300 (2006) e440–e443, https://doi.org/10.1016/j.jmmm.2005.10.187.

[13] M.N. Popova, Spectroscopy of compounds from the family of rare-earth orthoborates, J. Rare Earth 27 (2009) 607–611, https://doi.org/10.1016/S1002-0721(08)60298-7.

[14] B.Z. Malkin, private communication.